Available online at www.sciencedirect.com
SCIENCE DIRECT®
Biochemical Pharmacology 67 (2004) 1873–1886
Biochemical Pharmacology
www.elsevier.com/locate/biochempharm

Cell cycle- and protein kinase C-specific effects of resiniferatoxin and resiniferonol 9,13,14-*ortho*-phenylacetate in intestinal epithelial cells

Mark R. Frey[a], Jennifer A. Clark[a], Nicholas W. Bateman[a], Marcelo G. Kazanietz[b], Adrian R. Black[a], Jennifer D. Black[a,*]

[a]*Department of Pharmacology and Therapeutics, Roswell Park Cancer Institute, Elm and Carlton Streets, Buffalo, NY 14263, USA*
[b]*Department of Pharmacology, Center for Experimental Therapeutics, University of Pennsylvania School of Medicine, 816 Biomedical Research Building II/III, 421 Curie Blvd., Philadelphia, PA 19104-6160, USA*

Received 22 September 2003; accepted 3 February 2004

Abstract

We have previously reported that protein kinase C (PKC) signaling can trigger hallmark events of cell cycle withdrawal in intestinal epithelial cells, including downregulation of cyclin D1, induction of $p21^{Waf1/Cip1}$, and activation of the growth suppressor function of pocket proteins. In the current study, we compared the cell cycle- and PKC-specific effects of the vanilloid resiniferatoxin (RTX), its parent diterpene resiniferonol 9,13,14-*ortho*-phenylacetate (ROPA), and the PKC agonist PMA in the IEC-18 non-transformed intestinal crypt cell line. ROPA and PMA were found to produce strikingly similar alterations in cell cycle progression and PKC activity in IEC-18 cells, although PMA was approximately 1000-fold more potent in producing these effects. Both agents induced a transient PKC-dependent blockade in $G_1 \rightarrow S$ progression associated with transient downregulation of cyclin D1 and induction of $p21^{Waf1/Cip1}$. In contrast, RTX produced a prolonged PKC-independent cell cycle arrest in G_0/G_1 phase which was maintained for longer than 24 h. This arrest was vanilloid receptor-independent and associated with prolonged downregulation of cyclin D1 mRNA and protein, with little effect on levels of $p21^{Waf1/Cip1}$. Combined exposure to RTX and ROPA produced a sustained and complete cell cycle blockade in IEC-18 cells, associated with depletion of cyclin D1 and sustained enhancement of $p21^{Waf1/Cip1}$ levels. PMA, ROPA, RTX and the RTX/ROPA combination were capable of activating ERK1/2 signaling in IEC-18 cells, albeit with different kinetics. In contrast, only PMA and ROPA activated JNK1/2 and p38 in this system. Notably, some preparations of commercially obtained RTX produced effects indistinguishable from those of the RTX/ROPA combination, suggesting that certain batches of the compound may contain significant amounts of ROPA (or another PKC agonist activity). Together, these data demonstrate that structurally related compounds can produce similar cell cycle-specific effects but through distinct mechanisms. In addition, they add to a growing body of evidence that vanilloids can have antiproliferative effects in a variety of cell types.

Keywords: Cell cycle; Protein kinase C; Resiniferatoxin; Resiniferonol 9,13,14-*ortho*-phenylacetate; Cyclin D1; $p21^{Waf1/Cip1}$; MAPK

1. Introduction

Resiniferatoxin (RTX), isolated from the latex of the Moroccan cactus-like plant *Euphorbia resinifera*, combines the structural features of two classes of natural irritants, phorbol esters and vanilloids [1]. The structural similarity between RTX and phorbol esters indicates that it may bind and activate members of the PKC family, and RTX is currently marketed as a PKC agonist by several companies. A limited number of studies have reported PKC-specific effects of RTX both in vivo and in vitro. For example, a report comparing the ability of tumor-promoting (e.g. phorbol 12-myristate 13-acetate, PMA) and non-tumor-promoting (e.g. RTX) agents to activate PKC α, γ, δ, ε, ζ, and η indicated that RTX preferentially activates PKC α at concentrations ranging from 1 to 100 nM, while at 1 μM the other isozymes are activated as well [2]. Furthermore, nanomolar concentrations of RTX were shown to cause membrane translocation of PKC in dorsal root ganglion neurons, albeit through an indirect mechanism [3], and activation of PKC α signaling was implicated in

Abbreviations: BIM I, bisindolylmaleimide I; PKC, protein kinase C; PMA, phorbol 12-myristate 13-acetate; RTX, resiniferatoxin; ROPA, resiniferonol 9,13,14-*ortho*-phenylacetate; PDBu, phorbol 12,13-dibutyrate

* Corresponding author. Tel.: +1-716-845-5766; fax: +1-716-845-8857.
E-mail address: jennifer.black@roswellpark.org (J.D. Black).

0006-2952/$ – see front matter © 2004 Elsevier Inc. All rights reserved.
doi:10.1016/j.bcp.2004.02.006

RTX-induced alterations in microvascular permeability in an experimental model [4]. In contrast, a number of studies have demonstrated only marginal affinity of RTX toward members of the PKC family [5–8], likely due to the presence of a homovanillic acid substituent at position C20 in the phorbol nucleus [9], casting doubt on the ability of RTX to directly activate PKCs.

A possible explanation for the conflicting findings regarding the effects of RTX on PKCs is that deesterification of RTX yields its parent diterpene resiniferonol 9,13,14-*ortho*-phenylacetate (ROPA). ROPA has the structure of a PKC-binding phorbol ester, and has been shown to be approximately 10-fold more potent than RTX for PKC binding [10]. In keeping with other phorbol esters, ROPA has been shown to activate PKCs and to have weak tumor promoting activity [11]. In vitro studies have further demonstrated that ROPA preferentially activates the classical PKC isozymes [2].

In addition to its structural homology to phorbol esters, RTX also contains a (homo)vanillyl moiety that is homologous to capsaicin (8-methyl-*N*-vanillyl-6-nonenamide), the major pungent ingredient in hot chili peppers [1]. Like capsaicin, RTX acts as an agonist for the vanilloid receptor, a ligand-gated ion channel found on sensory neurons [1]. Although most studies of the actions of vanilloids have focused on their ability to activate the vanilloid receptor (and ultimately desensitize afferent sensory neurons involved in nociception [1]), a growing body of evidence indicates that capsaicin and its analogs (including RTX) also have vanilloid receptor-independent effects on cell growth/cell cycle progression and cell survival in certain cell types [12–17]. In this regard, it is interesting to note that capsaicin has chemopreventive effects in various tumor systems (including animal models of colon cancer) that are unrelated to its effects on the vanilloid receptor [18–22]. In contrast, to our knowledge the cell cycle-specific effects of ROPA have not been investigated.

We have previously reported that PKC signaling in intestinal epithelial cells can trigger a coordinated program of molecular events leading to cell cycle withdrawal into G_0 [23,24]. Activation of PKC α, δ, and ε, or PKC α alone, in the IEC-18 non-transformed rat intestinal crypt cell line results in rapid downregulation of cyclin D1, induction of Cip/Kip cyclin-dependent kinase inhibitors, and activation of the growth suppressor functions of members of the pocket protein family (i.e. pRb, p107, and p130). Maintenance of PKC-induced cell cycle arrest requires sustained PKC signaling [23,24] and prolonged activation of the ERK/MAPK pathway [25]. The physiological significance of these findings is supported by the demonstration that (a) PKC α and other PKC isozymes undergo membrane translocation/activation precisely at the point within intestinal crypts at which cells cease dividing [24,26], (b) the program of cell cycle regulatory events triggered by PKC activation in IEC-18 cells is representative of the changes seen coincident with growth arrest in intestinal crypts in situ [24,26], and (c) ERK activity has been shown to be maintained in post-mitotic cells of the intestinal villus [27].

In the present study, we compare the cell cycle- and PKC-specific effects of the PKC agonist PMA, the vanilloid RTX, and its parent diterpene ROPA in IEC-18 cells. Our data demonstrate, for the first time, that both RTX and ROPA have potent cell cycle inhibitory effects in these cells. While the effects of ROPA are PKC-dependent and transient, paralleling those of PMA, RTX produces a long-lasting PKC- and vanilloid receptor-independent cell cycle arrest in this system. Interestingly, combined exposure to RTX and ROPA produces a sustained and complete cell cycle blockade in IEC-18 cells. As seen with PMA treatment, RTX, ROPA and the RTX/ROPA combination activate ERK signaling in these cells. PMA and ROPA also activate JNK1/2 and p38 MAPKs in this system. Notably, some preparations of commercially obtained RTX used in this study produced effects indistinguishable from those of the RTX/ROPA combination, suggesting that certain batches of this agent may also contain significant amounts of ROPA (or a contaminant with PKC agonist activity).

2. Materials and methods

2.1. Reagents

Mouse monoclonal PKC α-specific antibody was purchased from Upstate Biotechnology, Inc. Rabbit anti-PKC δ (C-17), anti-PKC ε (C-15), anti-cyclin D1 (H-295), and anti-total ERK1/2 (C-14) antibodies, and goat anti-total p38 (C-20) antibody, were obtained from Santa Cruz Biotechnology. Mouse monoclonal anti-phospho-p44/p42 MAPK (E10) antibody, mouse anti-phospho-JNK1/2 antibody, rabbit anti-total JNK1/2 antibody, and rabbit anti-phospho-p38 antibody were purchased from Cell Signaling Technology. Mouse monoclonal anti-$p21^{Waf1/Cip1}$ (G3-245) antibody was obtained from BD Pharmingen. Horseradish peroxidase-conjugated rat anti-mouse, goat anti-rabbit, and donkey anti-goat secondary antibodies were purchased from Jackson Immuno Research Laboratories, Inc., Chemicon International, and Santa Cruz Biotechnology, respectively. The pan PKC inhibitor GF 109203X (BIM I) and the MEK inhibitor 1,4-diamino-2,3-dicyano-1,4-bis(2-aminophenylthio)-butadiene (U0126) were obtained from LC Laboratories and Alexis Biochemicals, respectively. PMA was from Sigma, PDBu was from Alexis Biochemicals, and ROPA was from LC Laboratories. Different lots of RTX were purchased from Alexis Biochemicals or LC Laboratories. Iodo-RTX was from LC Laboratories.

2.2. Intestinal epithelial cell culture

The IEC-18 cell line (American Type Culture Collection; #CRL-1589) is an immature, non-transformed cell

line derived from rat ileal epithelium [28]. IEC-18 cells grown in culture retain characteristics of proliferating intestinal crypt cells including the expression of a similar PKC isozyme profile (α, δ, ε, ζ, and ι). IEC-18 cells were maintained in Dulbecco's modified Eagle's medium (Gibco-BRL) supplemented with 4 mM glutamine, 5 μg/ml filtered insulin, and 5% fetal bovine serum (Intergen).

2.3. Drug treatments

IEC-18 cells in logarithmic phase of growth were treated with PMA, ROPA, RTX, Iodo-RTX, or RTX/ROPA combinations for various times as indicated. All drugs were dissolved in ethanol with a final concentration in the medium of ≤0.1%. Control cells were treated with vehicle alone for various times; since the vehicle had no effects on the various parameters examined, only representative control data are shown.

2.4. Inhibition of PKC or ERK signaling

Inhibition of PKC activity was achieved by pretreatment of IEC-18 cells for 30 min with 5 μM BIM I, a general inhibitor of the classical and novel PKC isozymes [29]. Depletion of the phorbol ester-responsive isozymes expressed in IEC-18 cells (PKC α, δ, and ε) was accomplished by exposing cells to 1 μM PDBu for 24 h as previously described [23,24]. Inhibition of ERK signaling was achieved by pretreatment of IEC-18 cells for 30 min with the MEK inhibitor U0126 (10 μM). The following solvents were used to prepare drug stock solutions: DMSO for BIM I and U0126 and ethanol for PDBu.

2.5. Flow cytometric analysis

Cultured IEC-18 cells were harvested by trypsinization, fixed overnight in 70% ethanol at 4 °C, and resuspended in 20 mM Tris, pH 7.5 containing 250 mM sucrose, 5 mM $MgCl_2$, 0.37% NP-40 (Sigma), and 0.04 mg/ml RNase A (Sigma). Cellular DNA was stained with 25 μg/ml propidium iodide (Sigma) in 0.05% sodium citrate and quantified using flow cytometry. Cell cycle analysis was performed using the Winlist and Modfit programs (Verity Software House).

2.6. Preparation of whole cell extracts

Subconfluent cultures of IEC-18 cells grown in 100 mm tissue culture plates were washed twice with phosphate-buffered saline at 4 °C. Cells were scraped into boiling SDS lysis buffer containing 10 mM Tris–HCl, pH 7.4 and 1% SDS (approximately 150 μl per plate) and solubilized by boiling for 5 min. Cellular DNA was sheared by passing the fresh lysate through a 27.5 gauge needle five times. Extracts were cleared by room temperature centrifugation at 12,000 × *g* for 10 min and boiled in Laemmli sample buffer (50 mM Tris–HCl, pH 6.8, 10% (v/v) glycerol (VWR), 2.5% SDS, 2 mM EDTA, 10 mM DTT, and 0.05% (w/v) Bromophenol Blue) [30] for 5 min prior to being subjected to SDS–PAGE and immunoblot analysis.

2.7. Subcellular fractionation

Partitioning of IEC-18 cell extracts into cytosolic (soluble) and membrane (particulate) fractions was performed as previously described [23,26]. Briefly, subconfluent cultures of IEC-18 cells were rinsed twice with phosphate-buffered saline at 4 °C and scraped into an extraction buffer containing 20 mM Tris–HCl, pH 7.5, 2 mM EDTA, 2 mM EGTA, 0.5 mg/ml digitonin, 10 mM NaF, 4 mM PMSF, 2 mM benzamidine, 10 μg/ml leupeptin, and 10 μg/ml aprotinin (digitonin buffer). Digitonin-soluble (cytosolic) and -insoluble (particulate) fractions were separated by ultracentrifugation at 4 °C for 40 min at 100,000 × *g*. Cytosolic proteins were precipitated with freshly prepared 10% TCA for 10 min on ice, washed in acetone, solubilized in 50 μl 100 mM NaOH, and neutralized by addition of 50 μl 100 mM HCl. Particulate fractions were incubated in 100 μl digitonin buffer containing 1% Triton X-100 (Sigma; Triton buffer). Membrane proteins were cleared by 30 min centrifugation at 4 °C (10,000 × *g*). Cytosolic and membrane fractions were then boiled in Laemmli sample buffer for 5 min and subjected to SDS–PAGE and immunoblot analysis.

2.8. Western blot analysis

Whole cell lysates (30 μg protein) or lysates containing either soluble or membrane-associated proteins (20 μg protein) were separated by SDS–PAGE [30] using 10% (for PKC isozymes), 12.5% (for phospho-JNK1/2, total JNK1/2, phospho-p38, and total p38), or 20% (for phospho-ERK1/2, total ERK1/2, cyclin D1, and $p21^{Waf1/Cip1}$) SDS–polyacrylamide minigels. Cellular proteins were then electrophoretically transferred to nitrocellulose membrane (Bio-Rad Laboratories; Hercules, CA). Blots were routinely stained with 0.1% Fast Green to ensure equal protein loading and even transfer. Membranes were blocked in Tris-buffered saline (TBS; 20 mM Tris–HCl and 137 mM NaCl, pH 7.6) containing 5% non-fat powdered Carnation milk and 0.1% Tween-20 (Sigma) (TBSt/milk) for 1 h at room temperature or overnight at 4 °C. Following blocking, membranes were incubated for 2 h at room temperature or overnight at 4 °C with primary antibody in TBSt/milk followed by six 5 min washes in TBSt/milk. Membranes were then incubated for 1 h at room temperature in TBSt/milk containing horseradish peroxidase-conjugated secondary antibody, followed by six 5 min washes with TBSt/milk and three 5 min washes in 1× TBS.

Bound horseradish peroxidase was detected using the Super-Signal CL system (Pierce). Primary antibody dilutions were as follows: 1:1000 for PKC δ, phospho-JNK1/2, total JNK1/2, and phospho-p38, and 1:2000 for PKC α, PKC ε, phospho-ERK1/2, total ERK1/2, total p38, cyclin D1, and $p21^{Waf1/Cip1}$. Secondary antibodies were used at 1:2000.

2.9. Northern blot analysis of cyclin D1 mRNA

Cells were treated with vehicle (ethanol) or RTX for 6 h and RNA was isolated using the RNAeasy system (Qiagen). RNA was separated on 1% agarose–formaldehyde gels and total RNA was detected by ethidium bromide fluorescence [31]. RNA was then transferred to Nytran nylon membrane (S&S). Following crosslinking, membranes were blocked with Quickhyb (Stratagene), and probed with [^{32}P]-labeled randomly primed cyclin D1 cDNA. Following high stringency washing, membranes were subjected to phosphorimaging and visualization/quantitation using the Storm/ImageQuant system (Molecular Diagnostics).

2.10. Statistical analysis

Statistical analysis of the differences between the cell cycle-specific effects of PMA (100 nM), ROPA (7.5 μM), and RTX (7.5 μM) was performed by two-tailed Student's *t*-test using Microsoft Excel Software. *P* values of less than 0.05 were considered significant.

3. Results

3.1. Comparison of the effects of PMA, ROPA, and RTX on IEC-18 cell cycle progression

To compare the cell cycle-specific effects of PMA, ROPA, and RTX in IEC-18 cells, asynchronously growing cell populations (in logarithmic phase of growth) were treated with various concentrations of these agents for various times and cellular DNA content/cell cycle distribution was determined by flow cytometric analysis. All three agents arrested cell cycle progression in IEC-18 cells, albeit with different potency and kinetics (Figs. 1 and 2). While PMA inhibited cell cycle progression at concentrations as low as 1–10 nM (Fig. 1A(i)), 5–7.5 μM ROPA or RTX was required to achieve similar growth arrest in this system (Figs. 1A(ii) and 2A). As shown in Fig. 1B(i), exposure of IEC-18 cells to ROPA at a concentration of 7.5 μM produced strikingly similar cell cycle perturbations to those induced by 100 nM PMA (identical results were seen with 5 and 10 μM ROPA, Fig. 1A(ii) and data not shown). A transient blockade in $G_1 \rightarrow S$ progression was observed by 6 h of treatment which was reversed by 12 h. Statistical analysis revealed no significant differences between the effects of PMA and ROPA at each time point examined (e.g. *P* values for the effects of these agents on S-phase were $\geq$0.95 for all time points except 12 h which was 0.8). Furthermore, as we have previously reported for PMA [24], ROPA induced a transient downregulation of cyclin D1 and a marked increase in $p21^{Waf1/Cip1}$ expression in these cells (Fig. 1B(ii)). Both PMA- and ROPA-induced downregulation of cyclin D1 was followed by a sustained hyperinduction of the protein.

In contrast to the effects of PMA and ROPA, treatment with RTX at 5–10 μM (data shown only for 7.5 μM, Fig. 2B(i)) produced a prolonged cell cycle arrest in G_0/G_1 phase that was first evident by 6 h and sustained for at least 24 h. Statistical analysis confirmed the differences in the effects of these agents since *P* values of <0.05 were obtained at each time point examined. Notably, the vanilloid receptor antagonist iodo-resiniferatoxin and RTX similarly affected IEC-18 cell cycle progression (Fig. 2B(ii)), indicating that the effects of these agents are independent of vanilloid receptor agonist activity. As shown in Fig. 2B(ii) and (iii), 7.5 μM RTX produced a sustained downregulation of cyclin D1 protein and mRNA expression in IEC-18 cells, but had little effect on $p21^{Waf1/Cip1}$ levels throughout the time course of the experiment.

3.2. Analysis of the PKC-dependence of the cell cycle-specific effects of PMA, ROPA, and RTX in IEC-18 cells

Two approaches were used to determine the PKC dependence of the cell cycle-specific effects of PMA, ROPA, and RTX in IEC-18 cells. First, cells were exposed to these agents in the presence of the PKC inhibitor BIM I, a general inhibitor of the classical and novel members of the PKC family [29]. Alternatively, phorbol ester-responsive isozymes (i.e. PKC α, δ, and ε) were depleted from the cells by treatment with 1 μM PDBu for 24 h [23]. Both PMA- and ROPA-induced IEC-18 cell cycle arrest was blocked by BIM I treatment (Fig. 3A), pointing to the requirement for PKC signaling in the negative growth regulatory effects of these agents. The cell cycle effects of PMA and ROPA were also inhibited by PKC depletion (data not shown). Consistent with these findings, both ROPA and PMA induced membrane translocation of PKC α, δ, and ε by 15 min of treatment (Fig. 3B). As we have previously described for PMA in IEC-18 cells [23], activation of these molecules by either agent was followed by their downregulation, accounting for the reversal of cell cycle arrest observed by ~12 h of treatment (see Fig. 1B(i)).

In contrast, analysis of the PKC-dependence of RTX-induced cell cycle effects in IEC-18 cells revealed that neither the PKC inhibitor BIM I (data not shown) nor PKC isozyme depletion from the cells by PDBu treatment prevented cell cycle arrest by this agent (Fig. 3C). Furthermore, cellular subfractionation experiments demonstrated

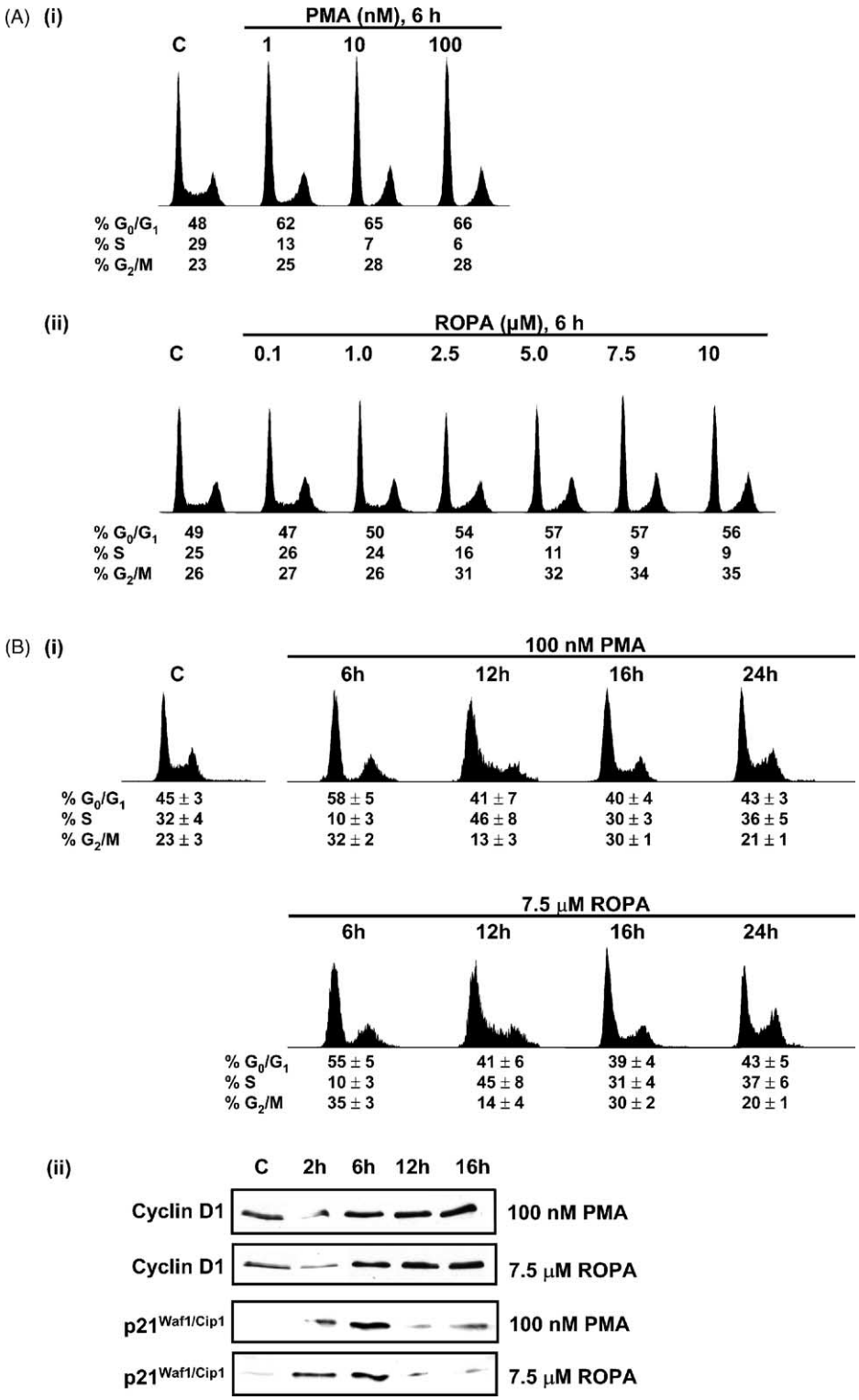

Fig. 1. Effects of PMA and ROPA on cell cycle progression and expression of cyclin D1 and $p21^{Waf1/Cip1}$ in IEC-18 cells. (A) IEC-18 cells were treated with PMA (i) or ROPA (ii) at various concentrations as indicated for 6 h, and DNA content/cell cycle distribution was determined by flow cytometric analysis. C: vehicle-treated cells. (B) IEC-18 cells were treated with either 100 nM PMA or 7.5 μM ROPA for the indicated times. (i) DNA content/cell cycle distribution was determined by flow cytometric analysis and (ii) expression of cyclin D1 and $p21^{Waf1/Cip1}$ was analyzed by Western blotting. C: representative control cells treated with vehicle (ethanol) alone for 6 h (i) or 2 h (ii). Data are representative of at least three independent experiments. Numbers in (i) are the averages of these experiments ± S.E. of the mean.

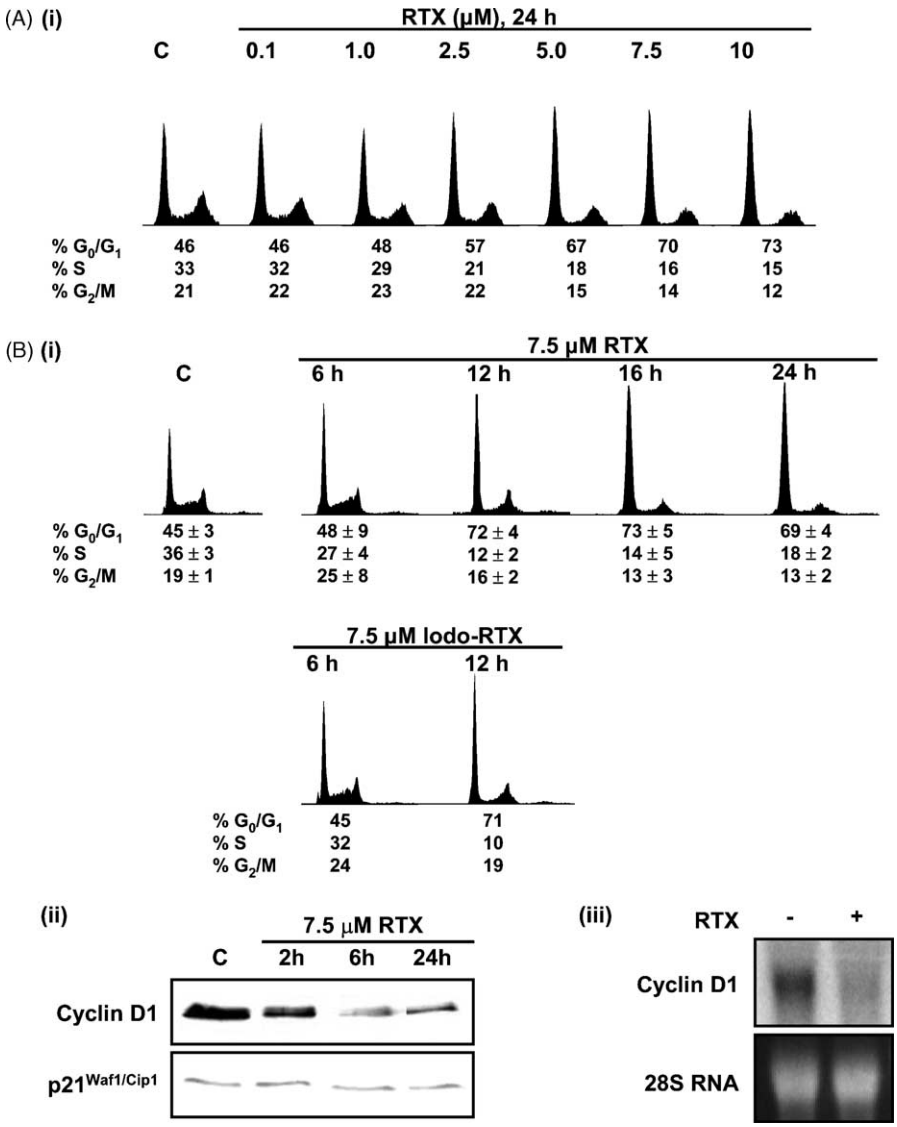

Fig. 2. Effects of RTX on cell cycle progression and cell cycle regulatory molecules in IEC-18 cells. (A) IEC-18 cells were treated with RTX at various concentrations as indicated for 24 h, and DNA content/cell cycle distribution was determined by flow cytometric analysis. C: vehicle-treated cells. (B) IEC-18 cells were treated with 7.5 μM RTX or 7.5 μM iodo-RTX, a vanilloid receptor antagonist, for the indicated times and effects on (i) cell cycle distribution and (ii) expression of cell cycle regulatory proteins were determined. (iii) Northern blot analysis of cyclin D1 expression in vehicle (ethanol)- or RTX-treated IEC-18 cells (6 h). C: representative control cells treated with vehicle (ethanol) alone for 6 h (i and iii) or 2 h (ii). Data are representative of at least three independent experiments, except for (iii) which is representative of two independent experiments. Numbers in (i) are the averages of these experiments ± S.E. of the mean.

that RTX is unable to induce membrane translocation of phorbol ester-responsive PKC isozymes in this system, either through direct or indirect mechanisms (Fig. 3D). Thus, consistent with reports that RTX performs poorly as a PKC ligand in vitro [5–8], RTX treatment induces IEC-18 cell cycle arrest through a PKC-independent mechanism.

3.3. Effects of combined exposure to RTX and ROPA on PKC activation and cell cycle progression in IEC-18 cells

Based on the finding that ROPA and RTX induce IEC-18 cell cycle arrest through different mechanisms, experiments were performed to examine the combined effects of these agents on (a) cell cycle progression, (b) expression of the cell cycle regulatory molecules cyclin D1 and $p21^{Waf1/Cip1}$, and (c) PKC activity in IEC-18 cells. Cells were treated with various combinations of RTX and ROPA and harvested for analysis at the indicated times. As shown in Fig. 4A, treatment with a combination of 7.5 μM RTX and 7.5 μM ROPA produced sustained cell cycle arrest (>24 h) in IEC-18 cells. Interestingly, while a small S phase population was consistently observed following 24 h treatment with RTX alone (e.g. 14% of the total in the experiment shown), the RTX/ROPA combination produced almost complete depletion of S phase cells (e.g. with

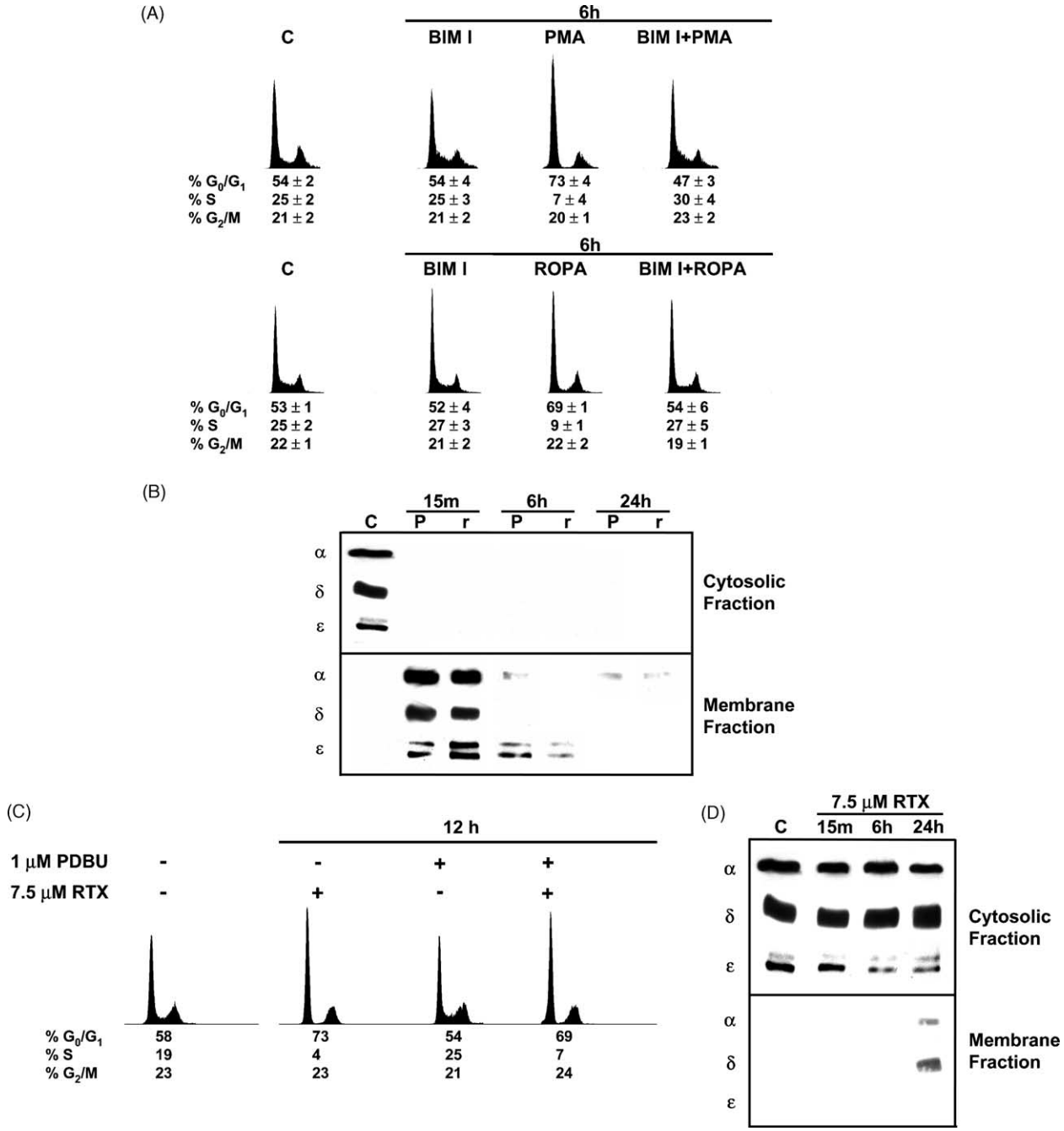

Fig. 3. Analysis of the PKC-dependence of the cell cycle-specific effects of PMA, ROPA and RTX in IEC-18 cells. (A) IEC-18 cells were treated with 100 nM PMA or 7.5 μM ROPA for 6 h in the absence or presence of the general PKC inhibitor BIM I (5 μM). Cell cycle distribution was determined by flow cytometric analysis. C: control cells treated with vehicle alone for 6 h. (B) Cytosolic and membrane subcellular fractions were prepared from PMA- and ROPA-treated IEC-18 cells and subjected to immunoblot analysis using antibodies specific for PKC α, δ, and ε. C: cells treated with vehicle alone for 15 min; P: PMA; r: ROPA. (C) Phorbol ester-responsive PKC isozymes were depleted from IEC-18 cells by 24 h incubation in 1 μM PDBu [23] and PKC-depleted cells were treated with 7.5 μM RTX for 12 h. Cell cycle distribution was determined by flow cytometric analysis. Control cells were treated with vehicle alone for 12 h. (D) IEC-18 cells were treated with 7.5 μM RTX for the indicated times and cytosolic and membrane fractions were analyzed for the expression of PKC α, δ, and ε. C: cells treated with vehicle alone for 15 min. Data in (A), (C) and (B), (D) are representative of at least three and two independent experiments, respectively. Numbers in (A) are the averages of these experiments ± S.E. of the mean.

<5% of cells remaining in this phase of the cell cycle; also, compare Figs. 2A, B and 4A). Western blot analysis demonstrated that the presence of RTX prevented the reappearance of cyclin D1 observed with ROPA alone in these cells (Fig. 4B). The combination of these agents also resulted in prolonged induction of the cyclin-dependent kinase inhibitor $p21^{Waf1/Cip1}$, which peaked before 10 h but was maintained for longer than 24 h (Fig. 4B).

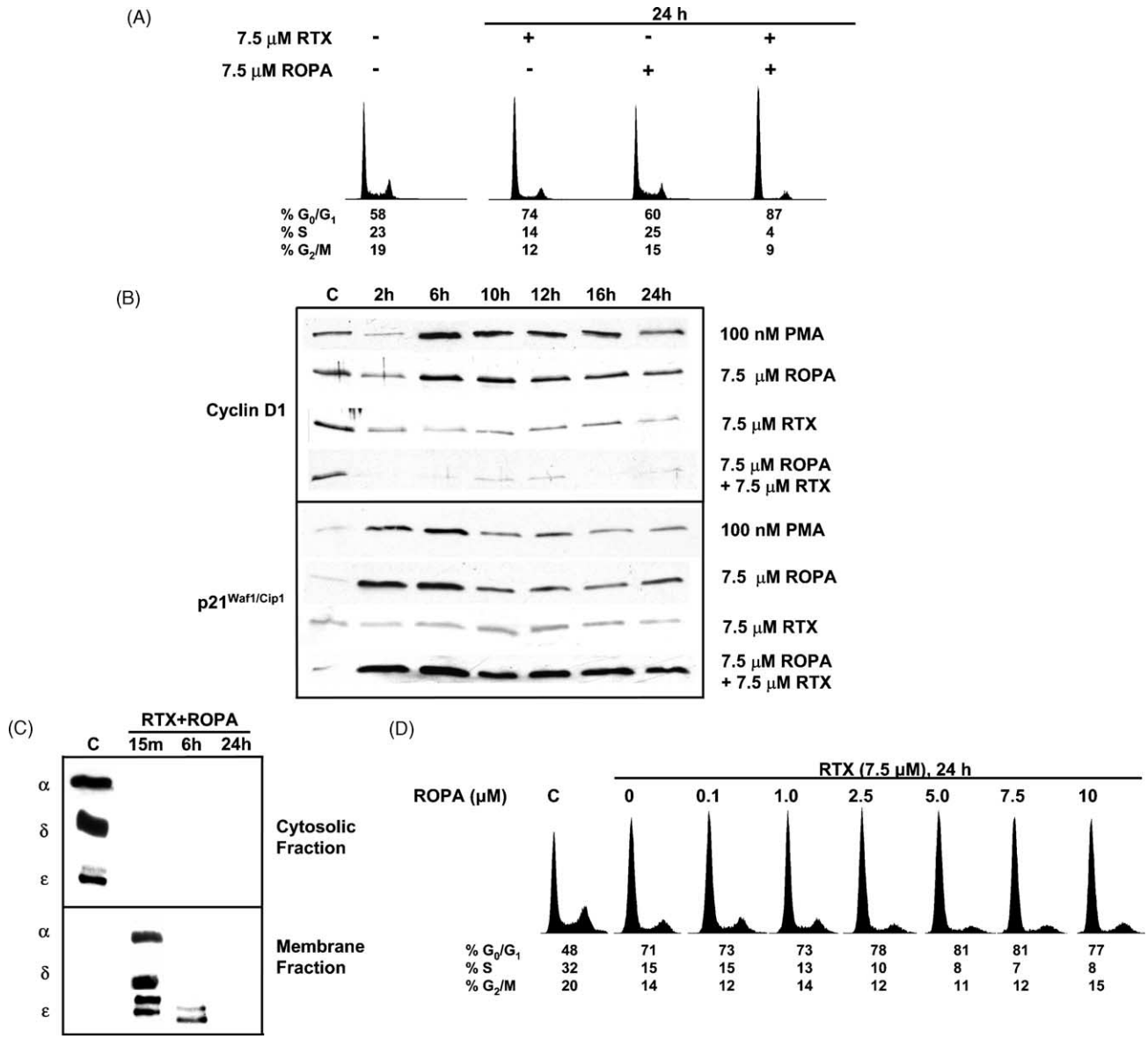

Fig. 4. Combined exposure to RTX and ROPA results in prolonged IEC-18 cell cycle arrest associated with sustained downregulation of cyclin D1/induction of $p21^{Waf1/Cip1}$ and activation of phorbol ester-responsive PKC isozymes. Asynchronously growing IEC-18 cells were treated with 7.5 μM RTX, 7.5 μM ROPA, or 7.5 μM RTX and 7.5 μM ROPA in combination for the indicated times. (A) Cell cycle distribution was determined by flow cytometric analysis and (B) expression of cyclin D1 and $p21^{Waf1/Cip1}$ was analyzed by Western blotting. C: representative control cells treated with vehicle alone for 24 h (A) or for 2 h (B). (C) IEC-18 cells were treated with 7.5 μM RTX and 7.5 μM ROPA in combination for the indicated times and cytosolic and membrane fractions were analyzed for the expression of PKC α, δ, and ε by Western blotting. C: cells treated with vehicle alone for 15 min. (D) IEC-18 cells were treated with RTX (7.5 μM) for 24 h in the absence or presence of various concentrations of ROPA as indicated. Cell cycle distribution was determined by flow cytometric analysis. C: vehicle-treated cells. Data in (A)–(D) are representative of at least three independent experiments.

The RTX/ROPA combination promoted membrane translocation and subsequent downregulation of PKC α, δ, and ε (Fig. 4C), paralleling the effects seen with ROPA alone (indeed, RTX does not appear to alter the overall effects of ROPA on PKC isozymes in this system; see Fig. 3B). The early peak (2–6 h) in $p21^{Waf1/Cip1}$ expression may thus reflect the strong input from PKC signaling at this time. Together, the data indicate that, by activating two independent pathways, a combination of RTX and ROPA produces a more complete and sustained IEC-18 cell cycle arrest than either agent alone, likely mediated by prolonged depletion of cyclin D1 and sustained enhancement of $p21^{Waf1/Cip1}$ expression in the cells.

To determine the concentration-dependence of the effects of ROPA on RTX-induced IEC-18 cell growth arrest, cells were exposed to RTX (7.5 μM) in the absence or presence of increasing concentrations of ROPA (100 nM–10 μM). As shown in Fig. 4D, at least 2.5 μM ROPA is required to modulate the cell cycle-specific effects of RTX in this system (an amount consistent with the concentration required for ROPA alone to alter IEC-18 cell cycle progression; Fig. 1A(ii)).

3.4. Involvement of the ERK signaling pathway in the cell cycle-specific effects of ROPA, RTX, and the RTX/ROPA combination in IEC-18 cells—comparison with PMA

It is now well recognized that ERK signaling can regulate two mutually antagonistic cellular processes, cell proliferation and cell cycle withdrawal/differentiation [32–34]. In IEC-18 cells, although treatment with the MEK inhibitor U0126 does not block cell cycle progression, it does reduce the percentage of cells in S phase, demonstrating the involvement of ERK signaling in promoting cell cycle progression in these cells [25]. Recent studies in our laboratory have further demonstrated that activation of the ERK pathway is also required for PKC agonist (i.e. PMA and bryostatin)-induced cyclin D1 downregulation, $p21^{Waf1/Cip1}$ induction, and cell cycle arrest in IEC-18 cells, and that the duration of these cell cycle effects correlates with the intensity/duration of ERK1/2 activation [25]. As shown in Fig. 5A, treatment of IEC-18 cells with ROPA, RTX, or a combination of these agents also promoted activation of the ERK pathway, as indicated by increased expression of the dually phosphorylated, activated form of ERK1/2. ROPA and PMA showed similar kinetics of ERK activation, with strong induction seen at early times of treatment, followed by a decline in ERK activity over the first 6 h and marked downregulation by 10 h. RTX generally induced a somewhat weaker activation of the ERK pathway, which was also reversed by 10 h. Interestingly, the RTX/ROPA combination, which produced the most complete and sustained growth arrest in IEC-18 cells, induced more intense and more prolonged activation of ERK1/2, with active phospho-ERK1/2 still detectable after 12 h of treatment.

The requirement for ERK activity in the cell cycle-specific effects of these agents was examined using the MEK inhibitor U0126. As shown in Fig. 5B, U0126 effectively blocked ERK1/2 phosphorylation (activation)

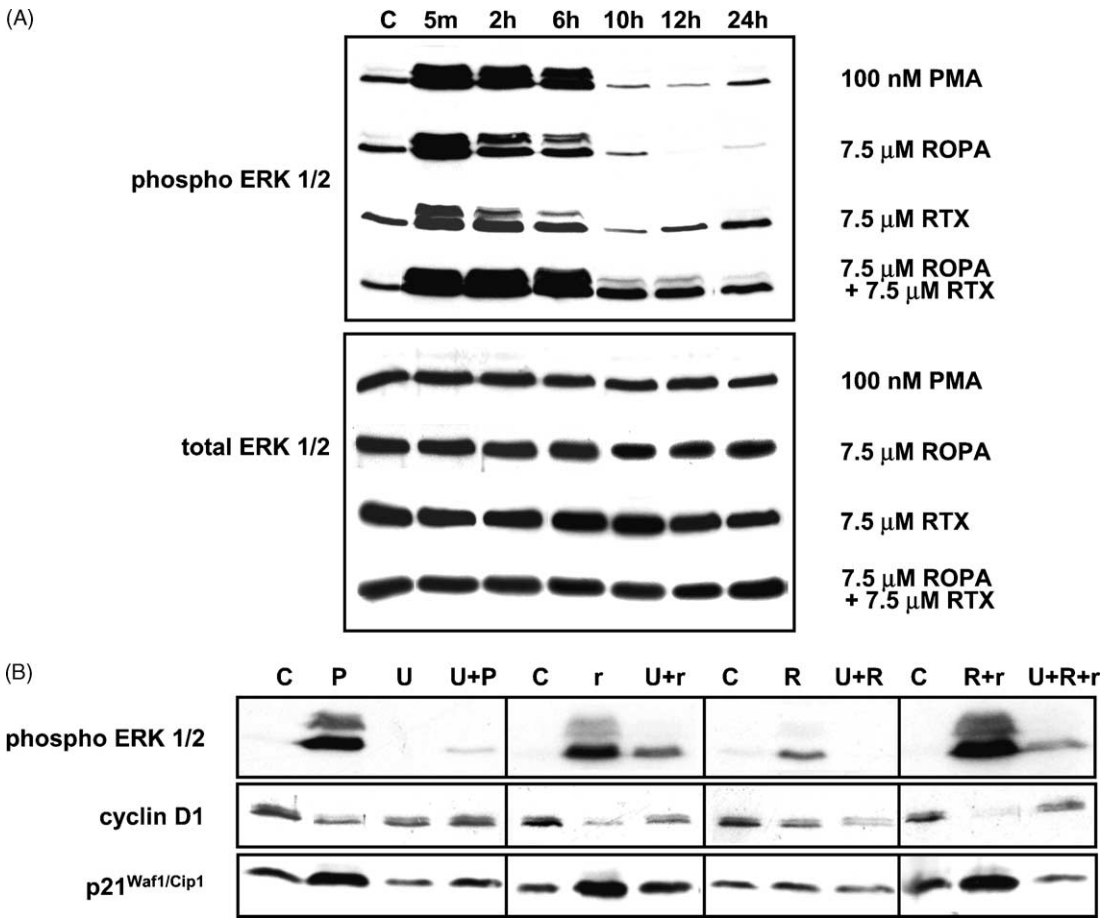

Fig. 5. Involvement of the ERK/MAPK pathway in the cell cycle-specific effects of PMA, RTX, ROPA, and the RTX/ROPA combination in IEC-18 cells. (A) Asynchronously growing IEC-18 cells were treated with 100 nM PMA, 7.5 μM RTX, 7.5 μM ROPA, or 7.5 μM RTX/7.5 μM ROPA for the indicated times, and whole cell lysates were prepared and subjected to immunoblot analysis using antibodies specific for the phosphorylated/active form of ERK1/2 and for total ERK1/2. C: representative control cells treated with vehicle alone for 5 min (note that phospho-ERK levels did not change significantly in vehicle-treated cells over the 24 h incubation period). (B) IEC-18 cells were treated with 100 nM PMA (P), 7.5 μM RTX (R), 7.5 μM ROPA (r), or 7.5 μM RTX/7.5 μM ROPA (R + r) for 2 h in the presence or absence of 10 μM U0126 (U). Whole cell lysates were prepared and ERK1/2 activation and cyclin D1/$p21^{Waf1/Cip1}$ expression were determined by immunoblot analysis. C: cells treated with vehicle alone for 2 h. Data in (A) and (B) are representative of at least two independent experiments.

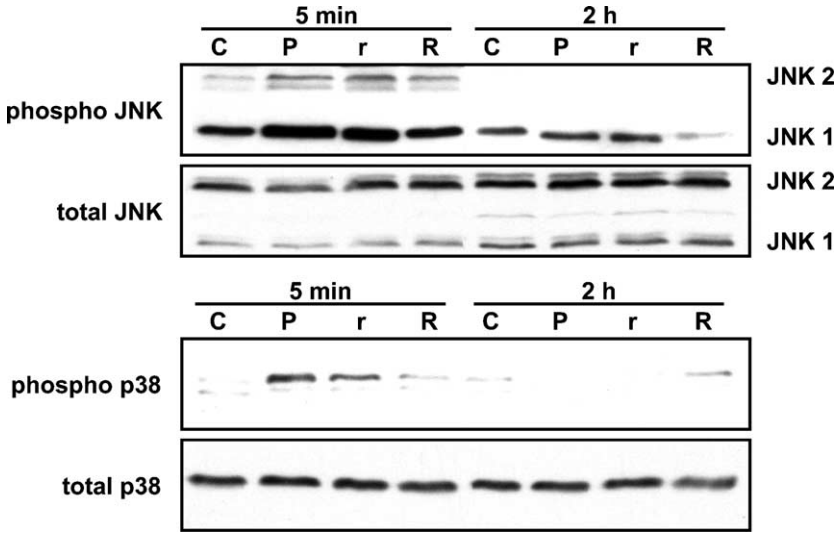

Fig. 6. Effects of PMA, ROPA, and RTX on the JNK1/2 and p38 signaling pathways in IEC-18 cells. IEC-18 cells were treated with 100 nM PMA (P), 7.5 μM ROPA (r), or 7.5 μM RTX (R) for 5 min or 2 h and whole cell lysates were subjected to immunoblot analysis using antibodies specific for the phophorylated/active forms of JNK1/2 or p38 and for total JNK1/2 or p38. C: vehicle-treated cells. Data are representative of three independent experiments.

in IEC-18 cells under all treatment conditions. Inhibition of ERK signaling prevented downregulation of cyclin D1 and induction of $p21^{Waf1/Cip1}$ by ROPA and PMA (Fig. 4B). In contrast, ERK inhibition did not prevent RTX-induced cyclin D1 downregulation in IEC-18 cells, pointing to the involvement of a different pathway of cyclin D1 regulation in cells treated with this agent. U0126 also partially inhibited the complete depletion of cyclin D1 by the RTX/ROPA combination, indicating that the effects on cyclin D1 expression produced by this treatment involved, at least in part, an ERK-dependent mechanism. Taken together, the data demonstrate that, like PMA [25], ROPA, RTX, and the RTX/ROPA combination are capable of activating ERK1/2 signaling in IEC-18 cells. While the effects of ROPA and PMA on cyclin D1 and $p21^{Waf1/Cip1}$ expression are ERK1/2-dependent, RTX-induced downregulation of cyclin D1 is ERK-independent. In the case of treatments that promote PKC signaling in this system (i.e. PMA, ROPA, RTX/ROPA), the intensity and duration of ERK activation correlate with the extent/duration of the growth arrest induced in the cells.

3.5. Differential effects of PMA, ROPA, and RTX on the activity of the MAPKs JNK and p38

To define further the differences between PMA, ROPA, and RTX with respect to IEC-18 cell cycle regulation, Western blot analysis was performed to determine the effects of these agents on the JNK1/2 and p38 signaling pathways. Fig. 6 demonstrates that, consistent with their parallel effects on PKC/ERK activity and cell cycle progression, both PMA and ROPA activated JNK1/2 and p38 in IEC-18 cells by 5 min of treatment. Phosphorylation/activation of these molecules was transient, with a return to baseline observed by 2 h. In contrast, RTX produced minimal effects on the phosphorylation/activation of either JNK1/2 or p38 in IEC-18 cells.

3.6. Effects on IEC-18 cell cycle progression and PKC activity vary among commercially obtained RTX preparations

During the course of this study, several commercial preparations of RTX were tested for their effects on IEC-18 cell cycle progression and PKC isozyme activation status. Notably, while the majority of these preparations were unable to induce membrane translocation of PKC α, δ, and ε in IEC-18 cells (see Fig. 3D), in some cases, newly purchased RTX samples produced effects indistinguishable from those seen with RTX/ROPA combinations. As shown in Fig. 7, such preparations (referred to as RTX-PKC) produced a complete and prolonged depletion of S phase cells (Fig. 7A), membrane translocation of phorbol ester-responsive isozymes (Fig. 7B), sustained activation of the ERK pathway, as well as prolonged downregulation of cyclin D1 and marked and sustained induction of $p21^{Waf1/Cip1}$ (Fig. 7C). These effects were strikingly similar to those seen in response to RTX and ROPA in combination (see Fig. 4). Based on the findings described in this study, we caution that some preparations of RTX are likely to also contain significant amounts of ROPA or a substance with similar effects on PKC.

4. Discussion

The current study demonstrates for the first time that both RTX and its parent diterpene ROPA can induce G_0/G_1

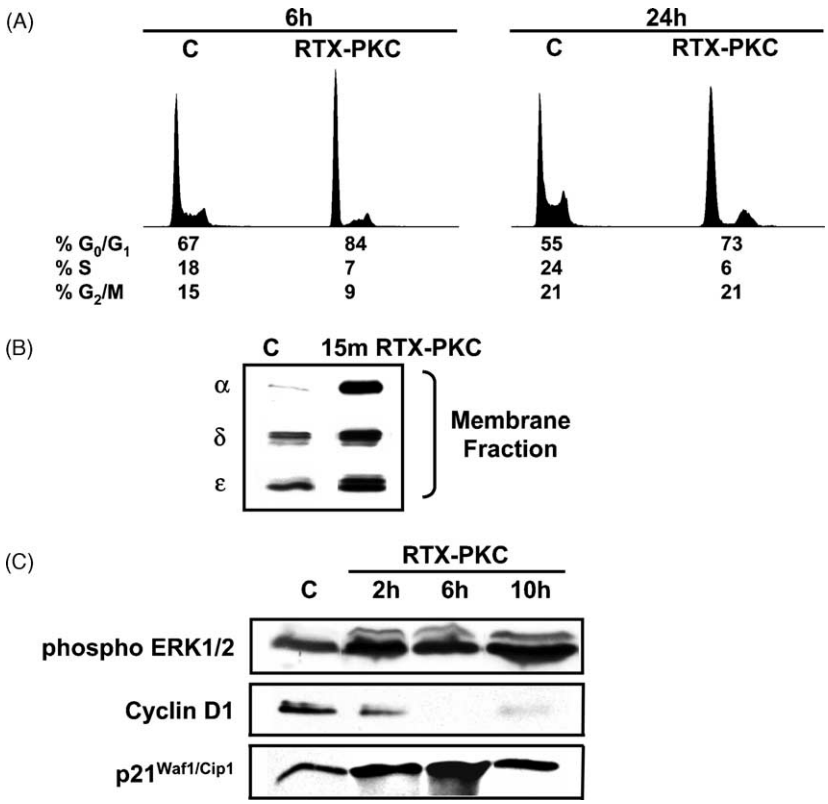

Fig. 7. Variable effects of RTX preparations on PKC activity and cell cycle progression in IEC-18 cells: some RTX preparations, referred to as RTX-PKC, produced effects similar to the RTX/ROPA combination in IEC-18 cells. (A) IEC-18 cells were treated with 10 μM RTX-PKC for 6 or 24 h and cell cycle distribution was determined by flow cytometric analysis. C; cells treated with vehicle alone. (B) IEC-18 cells were treated with 10 μM RTX-PKC for 15 min and membrane fractions were analyzed for the expression of PKC α, δ, and ε by Western blotting. C: cells treated with vehicle alone. (C) IEC-18 cells were treated with 10 μM RTX-PKC for the indicated times. Whole cell lysates were prepared and subjected to Western blot analysis using antibodies specific for the phosphorylated active form of ERK1/2, cyclin D1, and $p21^{Waf1/Cip1}$. C: representative control cells treated with vehicle alone for 2 h. Data in (A)–(C) are representative of three independent experiments.

arrest in non-transformed intestinal epithelial cells, albeit through different mechanisms. While ROPA-induced IEC-18 cell cycle arrest is PKC-dependent, RTX inhibits cell cycle progression through a PKC-independent pathway. Furthermore, ROPA produces ERK-dependent downregulation of cyclin D1 and induction of $p21^{Waf1/Cip1}$ expression in these cells, while RTX only affects cyclin D1 levels, in an ERK-independent manner. ROPA, but not RTX, also activates other members of the MAPK family including JNK1/2 and p38. Consistent with the involvement of different mechanisms, combined exposure to RTX and ROPA produces a more prolonged and complete cell cycle arrest in IEC-18 cells. Notably, the combination also produces a stronger and more prolonged activation of the ERK signaling pathway, combined with more complete downregulation of cyclin D1 and more sustained induction of $p21^{Waf1/Cip1}$.

4.1. PKC activation by RTX and ROPA in IEC-18 cells

RTX is marketed as a PKC agonist by several manufacturers. However, our findings that RTX does not promote membrane translocation of PKC isozymes in IEC-18 cells and that RTX-induced G_0/G_1 arrest in these cells is PKC-independent is consistent with a large body of evidence that, despite its structural similarity to phorbol esters, RTX binds members of the PKC family with very low affinity [5–8]. Thus, while one study [2] indicated that RTX could activate PKC α and other PKC isozymes in vitro, our results are in agreement with other studies which have shown that RTX is a very poor PKC ligand. Early work by Blumberg and Driedger [35,36] demonstrated that the compound is unable to evoke cellular responses characteristic of phorbol esters and that RTX does not compete effectively with PDBu for PKC binding in isolated membranes. Similarly, we have demonstrated that less than 20% inhibition of [^{3}H]-PDBu binding to PKC α, β, γ, δ, ε, η, and ζ can be achieved with RTX at a concentration of 10 μM [6]. In studies to determine the affinity of RTX for seven recombinant PKC isozymes (by competition for specific [^{3}H]-PDBu binding sites (30 nM)), Evans and coworkers reported IC_{50} values of 9 and 45 μM for the alternatively spliced PKC βI and βII isozymes, respectively, while other PKCs showed no binding to RTX [7]. Taken together, the data strongly support the notion that

RTX does not activate PKC in vitro or in vivo and should, therefore, not be considered a PKC agonist.

In contrast to RTX, ROPA (5–10 μM) produces robust membrane translocation and subsequent downregulation of PKC α, δ, and ε in IEC-18 cells. Thus, the diterpene ROPA can function as a PKC agonist in vivo, although with much less potency than PMA (which produces similar PKC-specific effects at a concentration of ≤100 nM). These findings are consistent with evidence that ROPA is a weak tumor promoter [11], that the critical C20 position involved in phorbol ester binding to PKC is occupied by a free hydroxyl group in this compound, and that ROPA can activate certain PKC isozymes, including PKC α, δ, and ε, in in vitro assays [2].

Our studies reveal a potential basis for the confusion regarding the PKC agonist functions of RTX. Three commercially obtained preparations of RTX produced effects on PKC activity and IEC-18 cell cycle progression very similar to those observed with the RTX/ROPA combination. Like the combination, these RTX preparations induced membrane translocation of PKC α, δ, and ε, strong and prolonged activation of the ERK signaling pathway, and complete and sustained inhibition of cell cycle progression (Fig. 7). Based on these findings, together with an understanding of the structure of RTX and of the methods used for RTX production, we propose that some RTX preparations also contain significant amounts of ROPA (or a contaminant with PKC agonist activity). Possible sources of ROPA in these preparations include (a) incomplete removal of ROPA following synthesis of RTX from ROPA in the laboratory, and (b) hydrolysis of RTX during synthesis or storage.

4.2. Cell cycle-specific effects of RTX and ROPA in IEC-18 cells

Studies presented here further demonstrate that both RTX and ROPA are able to inhibit $G_1 \rightarrow S$ phase progression in IEC-18 cells. However, these related compounds act through different mechanisms. The cell cycle-specific effects of ROPA are very similar to those of PMA, although at a ~1000-fold higher concentration of the compound. As seen with PMA, the cell cycle blockade produced by ROPA is PKC-dependent and transient, with reversal of the effect coinciding with agonist-induced downregulation of PKC isozyme(s) [23,24] (Fig. 1). ROPA and PMA also induce ERK-dependent cyclin D1 downregulation and $p21^{Waf1/Cip1}$ induction in IEC-18 cells, with identical kinetics, and transiently activate JNK1/2 and p38 in this system. The striking similarities in the effects of these agents strongly point to the involvement of common mechanisms. Although the specific PKC isozyme(s) involved in ROPA-induced IEC-18 cell cycle arrest remain to be determined, based on the similarity between the effects of PMA and ROPA in these cells, it is tempting to speculate that PKC α also plays a critical role in mediating the cell cycle-specific effects of this agent in this system [23–25].

In contrast to ROPA, the cell cycle blockade produced by RTX in IEC-18 cells is independent of PKC activation. RTX induces prolonged activation of ERK signaling (6–10 h), in a PKC-independent manner, as well as ERK-independent downregulation of cyclin D1 expression. Unlike ROPA, RTX produces minimal effects on JNK1/2 or p38 signaling in IEC-18 cells. The fact that equivalent concentrations of ROPA do not produce PKC-independent cell cycle effects in IEC-18 cells indicates that the effects of RTX are dependent on the vanilloid moiety of the molecule. In keeping with this idea, we have observed similar cell cycle effects following treatment of IEC-18 cells with the vanilloid capsaicin (ARB and NWB, unpublished data). However, these effects are independent of vanilloid receptor agonist activity, since they were also seen with the receptor antagonist, iodo-RTX. While several studies have demonstrated the ability of capsaicin to induce vanilloid receptor-independent G_0/G_1 arrest in certain cell types [12–15], to our knowledge, cell cycle-specific effects of RTX have only been described in one other study in which treatment of squamous cell carcinoma cells with RTX resulted in inhibition of $G_1 \rightarrow S$ phase progression [15]. Previous to the current study, vanilloid receptor-independent effects of capsaicin and RTX had only been observed in oncogenically-transformed cells (e.g. [12,13,37]); however, by characterizing effects of RTX in IEC-18 cells, our study clearly indicates that such effects can also occur in non-transformed cells. The effects of vanilloids, including RTX, on transformed cells have been attributed to multiple mechanisms, including suppression of a plasma membrane NADH-oxidase, alterations in mitochondrial function, and inhibition of NF-κB activity [22]. In addition, RTX is able to stimulate the activity of a Ca^{2+}-inhibited and phosphatidylserine-dependent Rx-kinase [8]. Whether one or more of these mechanisms play a role in the antiproliferative effects of RTX in IEC-18 cells remains to be determined.

Complete and prolonged IEC-18 cell cycle arrest was achieved with the RTX/ROPA combination. Combined exposure to these agents results in stronger and more sustained ERK activation relative to either treatment alone, consistent with the notion that the strength and/or duration of the ERK signal can play a key role in determining cellular response to activation of this pathway [33,34,38]. This treatment also produces complete and prolonged depletion of cyclin D1; RTX thus appears to prevent the hyperinduction of cyclin D1 associated with PKC agonist-induced PKC depletion in IEC-18 cells [24]. In addition, the RTX/ROPA combination promotes strong and prolonged induction of $p21^{Waf1/Cip1}$. Since $p21^{Waf1/Cip1}$ levels are not affected by RTX, this finding supports a role for crosstalk between PKC- and RTX-induced pathways in producing prolonged induction of this protein. The presence of high levels of $p21^{Waf1/Cip1}$ may account for the

more complete growth inhibition induced by the combination.

In summary, both RTX and ROPA have antiproliferative effects in intestinal epithelial cells, albeit via different mechanisms. RTX-induced G_0/G_1 arrest in these cells is PKC-independent, adding to a large body of evidence indicating that this agent does not function as a PKC agonist. In contrast, ROPA-induced inhibition of $G_1 \rightarrow S$ phase progression is PKC-dependent, consistent with its ability to activate PKC isozymes in IEC-18 cells. The involvement of different mechanisms in the antiproliferative effects of RTX and ROPA is further supported by the finding that combined treatment of intestinal epithelial cells with these agents produces a more complete and prolonged G_0/G_1 arrest compared with either agent alone in this system. Finally, caution should be exercised in the use of RTX preparations which may contain undefined levels of ROPA (or another PKC agonist activity). Future studies will further investigate the molecular mechanisms underlying the antiproliferative effects of RTX in intestinal epithelial cells.

Acknowledgments

The authors wish to thank Laura Kunneva for expert technical assistance and Dr. Janice Sufrin for helpful discussions. This work was supported by NIH grants DK54909, DK60632, and CA16056 and by grants from the Mae Stone Goode Foundation and the Roswell Park Alliance Foundation.

References

[1] Szallasi A, Blumberg PM. Vanilloid (Capsaicin) receptors and mechanisms. Pharmacol Rev 1999;51:159–212.
[2] Geiges D, Meyer T, Marte B, Vanek M, Weissgerber G, Stabel S, et al. Activation of protein kinase C subtypes alpha, gamma, delta, epsilon, zeta, and eta by tumor-promoting and nontumor-promoting agents. Biochem Pharmacol 1997;53:865–75.
[3] Harvey JS, Davis C, James IF, Burgess GM. Activation of protein kinase C by the capsaicin analogue resiniferatoxin in sensory neurones. J Neurochem 1995;65:1309–17.
[4] Northover AM, Northover BJ. Stimulation of protein kinase C activity may increase microvascular permeability to colloidal carbon via alpha-isoenzyme. Inflammation 1994;18:481–7.
[5] Szallasi A, Blumberg PM. Specific binding of resiniferatoxin, an ultrapotent capsaicin analog, by dorsal root ganglion membranes. Brain Res 1990;524:106–11.
[6] Kazanietz MG, Areces LB, Bahador A, Mischak H, Goodnight J, Mushinski JF, et al. Characterization of ligand and substrate specificity for the calcium-dependent and calcium-independent protein kinase C isozymes. Mol Pharmacol 1993;44:298–307.
[7] Dimitrijevic SM, Ryves WJ, Parker PJ, Evans FJ. Characterization of phorbol ester binding to protein kinase C isotypes. Mol Pharmacol 1995;48:259–67.
[8] Sharma P, Ryves WJ, Gordge PC, Evans AT, Shaun N, Thomas B, et al. Properties of a resiniferatoxin-stimulated, calcium inhibited but phosphatidylserine-dependent kinase, which is distinct from protein kinase C isotypes alpha, beta 1, gamma, delta, epsilon and eta. J Pharm Pharmacol 1995;47:297–306.
[9] Jeffrey AM, Liskamp RM. Computer-assisted molecular modeling of tumor promoters: rationale for the activity of phorbol esters, teleocidin B, and aplysiatoxin. Proc Natl Acad Sci USA 1986;83:241–5.
[10] Szallasi A, Joo F, Blumberg PM. Duration of desensitization and ultrastructural changes in dorsal root ganglia in rats treated with resiniferatoxin, an ultrapotent capsaicin analog. Brain Res 1989;503:68–72.
[11] Hergenhahn M, Furstenberger G, Opferkuch HJ, Adolf W, Mack H, Hecker E. Biological assays for irritant tumor-initiating and -promoting activities. I. Kinetics of the irritant response in relation to the initiation-promoting activity of polyfunctional diterpenes representing tigliane and some daphnane types. J Cancer Res Clin Oncol 1982;104:31–9.
[12] Morre DJ, Sun E, Geilen C, Wu LY, de Cabo R, Krasagakis K, et al. Capsaicin inhibits plasma membrane NADH oxidase and growth of human and mouse melanoma lines. Eur J Cancer 1996;32A:1995–2003.
[13] Morre DJ, Chueh PJ, Morre DM. Capsaicin inhibits preferentially the NADH oxidase and growth of transformed cells in culture. Proc Natl Acad Sci USA 1995;92:1831–5.
[14] Lee YS, Nam DH, Kim JA. Induction of apoptosis by capsaicin in A172 human glioblastoma cells. Cancer Lett 2000;161:121–30.
[15] Hail Jr N, Lotan R. Examining the role of mitochondrial respiration in vanilloid-induced apoptosis. J Natl Cancer Inst 2002;94:1281–92.
[16] Zhang J, Nagasaki M, Tanaka Y, Morikawa S. Capsaicin inhibits growth of adult T-cell leukemia cells. Leuk Res 2003;27:275–83.
[17] Macho A, Sancho R, Minassi A, Appendino G, Lawen A, Munoz E. Involvement of reactive oxygen species in capsaicinoid-induced apoptosis in transformed cells. Free Radic Res 2003;37:611–9.
[18] Yoshitani SI, Tanaka T, Kohno H, Takashima S. Chemoprevention of azoxymethane-induced rat colon carcinogenesis by dietary capsaicin and rotenone. Int J Oncol 2001;19:929–39.
[19] Yun TK. Update from Asia. Asian studies on cancer chemoprevention. Ann NY Acad Sci 1999;889:157–92.
[20] Surh YJ, Han SS, Keum YS, Seo HJ, Lee SS. Inhibitory effects of curcumin and capsaicin on phorbol ester-induced activation of eukaryotic transcription factors, NF-kappaB and AP-1. Biofactors 2000;12:107–12.
[21] Surh YJ, Lee SS. Capsaicin, a double-edged sword: toxicity, metabolism, and chemopreventive potential. Life Sci 1995;56:1845–55.
[22] Surh YJ. More than spice: capsaicin in hot chili peppers makes tumor cells commit suicide. J Natl Cancer Inst 2002;94:1263–5.
[23] Frey MR, Saxon ML, Zhao X, Rollins A, Evans SS, Black JD. Protein kinase C isozyme-mediated cell cycle arrest involves induction of p21(waf1/cip1) and p27(kip1) and hypophosphorylation of the retinoblastoma protein in intestinal epithelial cells. J Biol Chem 1997;272:9424–35.
[24] Frey MR, Clark JA, Leontieva O, Uronis JM, Black AR, Black JD. Protein kinase C signaling mediates a program of cell cycle withdrawal in the intestinal epithelium. J Cell Biol 2000;151:763–78.
[25] Clark JA, Black AR, Leontieva OV, Frey MR, Pysz MA, Kunneva L, et al. Involvement of the ERK signaling cascade in protein kinase C-mediated cell cycle arrest in intestinal epithelial cells. J Biol Chem 2004;279:9233–47.
[26] Saxon ML, Zhao X, Black JD. Activation of protein kinase C isozymes is associated with post-mitotic events in intestinal epithelial cells in situ. J Cell Biol 1994;126:747–63.
[27] Aliaga JC, Deschenes C, Beaulieu JF, Calvo EL, Rivard N. Requirement of the MAP kinase cascade for cell cycle progression and differentiation of human intestinal cells. Am J Physiol 1999;277: G631–41.
[28] Quaroni A, May RJ. Establishment and characterizaton of intestinal epithelial cell cultures. Methods Cell Biol 1980;21B:403–27.
[29] Toullec D, Pianetti P, Coste H, Bellevergue P, Grand-Perret T, Ajakane M, et al. The bisindolylmaleimide GF 109203X is a potent and selective inhibitor of protein kinase C. J Biol Chem 1991;266:15771–81.

[30] Laemmli UK. Cleavage of structural proteins during the assembly of the head of bacteriophage T4. Nature 1970;227:680–5.
[31] Black AR, Dolnick BJ. Expression of rTS correlates with altered growth regulation of thymidylate synthase. Cancer Res 1996;56:700–5.
[32] Marshall CJ. Specificity of receptor tyrosine kinase signaling: transient versus sustained extracellular signal-regulated kinase activation. Cell 1995;80:179–85.
[33] Chen Z, Gibson TB, Robinson F, Silvestro L, Pearson G, Xu B, et al. Chem Rev 2001;101:2449–76.
[34] Cobb MH, Goldsmith EJ. How MAP kinases are regulated. J Biol Chem 1995;270:14843–6.
[35] Driedger PE, Blumberg PM. Different biological targets for resiniferatoxin and phorbol 12-myristate 13-acetate. Cancer Res 1980;40:1400–4.
[36] Driedger PE, Blumberg PM. Specific binding of phorbol ester tumor promoters. Proc Natl Acad Sci USA 1980;77:567–71.
[37] Macho A, Calzado MA, Munoz-Blanco J, Gomez-Diaz C, Gajate C, Mollinedo F, et al. Selective induction of apoptosis by capsaicin in transformed cells: the role of reactive oxygen species and calcium. Cell Death Differ 1999;6:155–65.
[38] Lewis TS, Shapiro PS, Ahn NG. Signal transduction through MAP kinase cascades. Adv Cancer Res 1998;74:49–139.